Available online at www.sciencedirect.com
ScienceDirect
Journal of Power Sources 163 (2006) 371–375
JOURNAL OF POWER SOURCES
www.elsevier.com/locate/jpowsour

Short communication

Effect of support on the activity of Pd electrocatalyst for ethanol oxidation

Hai Tao Zheng [a,b], Yongliang Li [b], Shuixia Chen [a], Pei Kang Shen [b,*]

[a] *Materials Science Institute, School of Chemistry and Chemical Engineering, Sun Yat-Sen University, Guangzhou 510275, PR China*
[b] *State Key Laboratory of Optoelectronic Materials and Technologies, School of Physics and Engineering, Sun Yat-Sen University, Guangzhou 510275, PR China*

Received 17 August 2006; received in revised form 21 September 2006; accepted 21 September 2006
Available online 3 November 2006

Abstract

Pd nanoparticles were supported on different types of the carbon materials including multiwall carbon nanotube (MWCNT), carbon black and activated carbon fiber (ACF) prepared by the intermittent microwave heating (IMH) technique. Different electrochemical techniques were employed to characterize the catalytic activities of the Pd-based electrocatalysts for ethanol oxidation in comparison with the Pt/C electrocatalyst. Pd supported on multiwall carbon nanotube (Pd/MWCNT) electrocatalyst showed the best performance for ethanol oxidation in alkaline media. An over 100 mV negative shift of the onset potential for ethanol oxidation was found on Pd/MWCNT compared to that on Pt/C. The results indicated that the support would significantly influence the catalytic activities of the Pd-based electrocatalysts for ethanol oxidation.

Keywords: Ethanol oxidation; Pd/MWCNT; Electrocatalyst; Fuel cells; Anode

1. Introduction

Direct ethanol fuel cells (DEFCs) have attracted more attention because ethanol has no toxicity, greater energy density (8.01 kWh kg^{-1}) and higher safety in operation compared to methanol. It can be easily produced in great quantity by the fermentation of sugar-containing raw materials [1,2]. However, the low reaction kinetics of ethanol oxidation is still a challenge. The oxidation of ethanol is more sluggish than that of methanol on Pt-based electrocatalysts in acidic media [3–6]. Lamy's group showed that PtRuSn/C and PtSn/C are very efficient electrocatalysts for the oxidation of ethanol [7]. Our previous work showed that the performance of the ethanol oxidation could be significantly improved in alkaline media even on the Pt-free electrocatalysts [8,9]. It is obvious that Pt is very costly and its supply is limited. In fuel cell, the high loading of expensive Pt on carbon has severely limited their use. Therefore, it is a need to develop low Pt loading or Pt-free electrocatalysts.

Here, we report the effect of support on the performance of Pd-based electrocatalysts for ethanol oxidation. High surface area carbon is usually used as the support to uniformly disperse metal electrocatalysts and consequently increase the metal utilization. Carbon nanotubes (CNTs) are of interest as catalyst supports for applications in fuel cells due to their unique electrical and structural properties [10–12]. Multiwall carbon nanotubes (MWCNTs) have been used as the support of the cathode electrocatalyst and showed a better performance in DEFCs than that of the cathode electrocatalysts supported on carbon black [13,14]. Recently, activated carbon fiber (ACF) was developed as a new material and has great potential as a catalyst support and as a adsorbent for pollution control because of their extended surface area, high adsorption capacity, fast adsorption/desorption rate, microporous structure and special surface reactivity [15,16]. In this study, MWCNT, ACF and carbon black were used as supports to prepare Pd-based electrocatalysts and compare their performance for ethanol oxidation.

2. Experimental

2.1. Pretreatment of the carbon materials

0.1 g MWCNT with tube diameters of 20–40 nm and purity >95% (Shenzhen Nanotech. Co., Ltd., China) were mixed with 60 ml of solution of 98%H_2SO_4 and 65%HNO_3 (1:1 by volume) under constant stirring for 15 min and then refluxed at

* Corresponding author. Tel.: +86 20 84036736; fax: +86 20 84113369.
E-mail address: stdp32@zsu.edu.cn (P.K. Shen).

0378-7753/$ – see front matter © 2006 Elsevier B.V. All rights reserved.
doi:10.1016/j.jpowsour.2006.09.062

140 °C for 4 h. The acid treated MWCNT was rinsed thoroughly using distilled-deionized water until neutral and dried at 80 °C for 24 h [17]. ACF was prepared as reported previously [18]. ACF (0.1 g) was mixed with 60 ml of a 1 mol l^{-1} HNO_3 solution under constant stirring for 3 h. The treated ACF was washed by distilled-deionized water and then dried at 80 °C for 24 h. Carbon black (Vulcan XC-72R, Cabot Corp., USA) was treated by the same procedure as that of ACF.

2.2. Synthesis of the electrocatalysts

Palladium electrocatalysts supported on MWCNT or carbon black or ACF were synthesized by the intermittent microwave heating (IMH) technique [19]. Fifty milligram MWCNT or C or ACF were mixed with 10 ml of 2-propanol under ultrasonic treatment for 20 min; 5.3 ml $PdCl_2$ solution (3.8 mgPd^{2+} ml^{-1}) was then slowly added into the MWCNT or C or ACF dispersion, followed by the ultrasonic treatment for 30 min (ultrasonic frequency is 40 kHz). After evaporation of the solvent, the thermal treatment of the sample was accomplished by using microwave irradiation (Galanz, WD900ASL23-2, China, 900 W, 2.45 GHz). The procedure was 5 s irradiation on and 60 s irradiation off for six times. The resulted sample was further treated for complete reduction of the metal salt to the metal. The sample was dispersed in formic acid (10 ml, 1.0 mol l^{-1} HCOOH). The dispersion was then put into a microwave oven and argon gas was supplied for 15 min to remove oxygen. The oxygen-free solution was heated under argon atmosphere in a procedure of 20 s irradiation on and 60 s irradiation off until the sample was completely dried. The loadings of Pd on MWCNT or C or ACF were 40 wt%, which was stoichiometricly calculated without further analysis.

2.3. Preparation of the electrodes

Typically, 1 mg 40 wt%Pd/MWCNT or 40 wt%Pd/C or 40 wt%Pd/ACF powders were dispersed in 2 ml 2-propanol with 5 wt% Nafion solution (DuPont, USA) (2-propanol:Nafion = 20:1) under ultrasonic stirring. The well-mixed electrocatalyst ink was then deposited on the surface of a graphite rod with the geometric area of 0.30 cm^2 and dried at 80 °C for 30 min. The Pd loadings on each electrode were normally controlled at 0.2 mg cm^{-2}.

2.4. Characterization of the electrocatalyst

X-ray diffraction (XRD) was employed to obtain the information of the surface and bulk structure of the electrocatalysts and was carried out with a D/MAX2200 diffractometer employing Cu Kα radiation (λ = 0.15418 nm). Transmission electron microscopic (TEM) measurement was performed with a Philips CM-300 high-resolution system operating at 200 keV. The morphologies of the eletrocatalysts were investigated by scanning electron microscopy (SEM) (LEO-1530VP, Germany, operating at 20 kV).

The electrochemical experiments were conducted in a standard three-electrode cell using IM6e electrochemical workstation (Zahner-Electrik, Germany) controlled at room temperature. A platinum foil (3.0 cm^2) and Hg/HgO (1.0 mol l^{-1} KOH) were used as counter and reference electrodes, respectively.

3. Results and discussion

Fig. 1 shows the morphologies of Pd/MWCNT, Pd/C and Pd/ACF electrocatalysts. It can be seen that all the supports keep the original shapes after deposited Pd electrocatalyst. The aggregation of Pd/C resulted in larger particles in micrometer scale. TEM observation (Fig. 2) found that Pd nanoparticles were dispersed on the surface of the MWCNT and the particles are ranging from 3 to 6 nm. It is noted that Pd particles are greater on the MWCNT bundles. This resulted from the greater amount of the carboxylic acid groups on the surface of the bundles due to the aggregate effect [20]. For Pd/C composites, the Pd nanoparticles are around 7–12 nm that are bigger than that on MWCNT (Fig. 2b). Pd on ACF shows a more uniform distribution (Fig. 2c), however, the Pd particles are even bigger than that on MWCNT under the same preparation conditions. The fact that the different particle sizes on different carbon supports means that the Pd deposition relates to the surface chemistry of the support and the experimental conditions. The optimization of the preparation conditions is in progress.

Fig. 3 shows the XRD patterns of Pd-based electrocatalysts. The main diffraction peaks of Pd nanoparticles were observed. All peaks can be indexed as Pd cubic crystallite. The crystalline peaks of Pd are very sharp in Pd/ACF. The Pd (1 1 1) peak was used to calculate the particle size of Pd according to the Scherrer equation and gave the average size of 4 nm for Pd/MWCNT, 8 nm for Pd/C and 10 nm for Pd/ACF, which are in agreement with the results from the TEM measurements.

The cyclic voltammograms of ethanol oxidation on Pd/MWCNT, Pd/C, Pd/ACF and commercial Pt/C are presented in Fig. 4. The inset in Fig. 4 is the CVs of Pd/MWCNT, Pd/C and Pd/ACF in 1 mol l^{-1} KOH solution without added ethanol. The scan rate was 50 mV s^{-1} in the potential range of −0.8 to 0.3 V versus Hg/HgO. The hydrogen adsorption/desorption peaks can be observed from the inset in Fig. 4. The hydrogen adsorption/desorption peaks were used to estimate the electrochemical active area (EAA) of the electrocatalyst. It is obvious that the EAA of the Pd/MWCNT is much larger than those on Pd/C and Pd/ACF due to the better dispersion of Pd and the porous structure. The order of the EAA values of hydrogen adsorption/desorption peaks is Pd/MWCNT > Pd/C > Pd/ACF. By comparing with the CVs in the inset, the ethanol shows distinguished oxidation peaks, but the hydrogen absorption/desorption peaks are greatly depressed duo to the competitive adsorption of ethanol molecules and hydrogen molecules. It implies that those ethanol molecules are absorbed preferably on the electrode surface in this potential region and inhibits the hydrogen adsorption on the electrode surface.

As can be seen from Fig. 4, the Pd-based electrocatalyst shows a higher peak current density. The higher peak current density contributed from the higher active surface area. The onset potential of ethanol oxidation on Pd/MWCNT is over

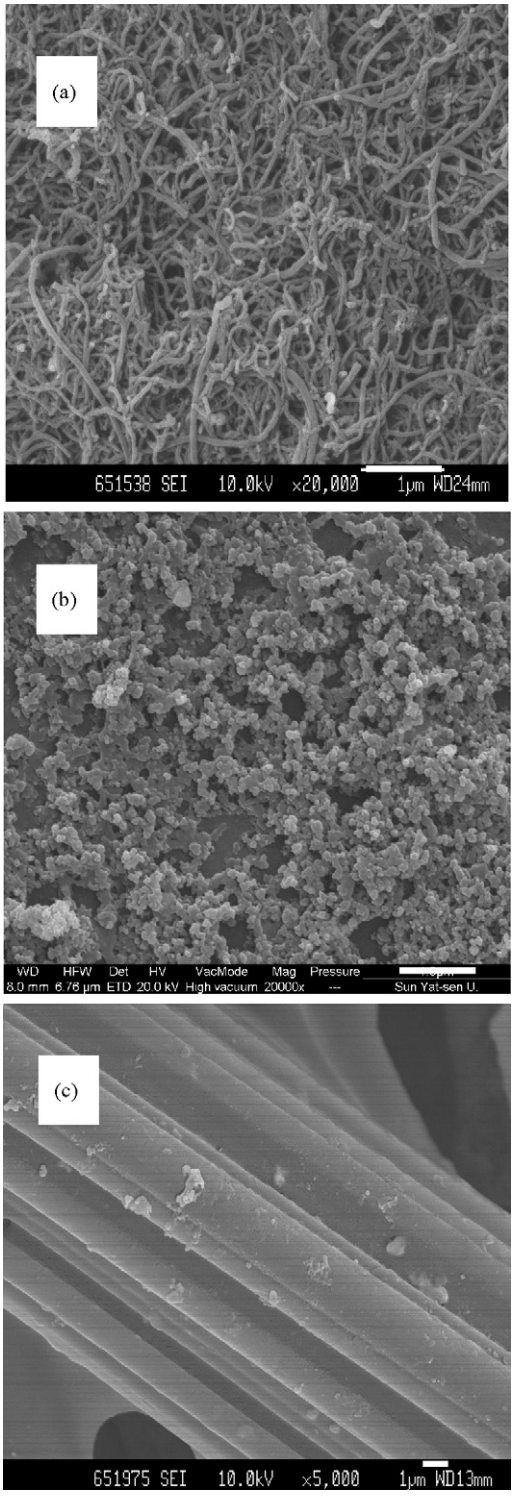

Fig. 1. SEM micrographs of (a) Pd/MWCNT, (b) Pd/C and (c) Pd/ACF. Bar: 1 μm.

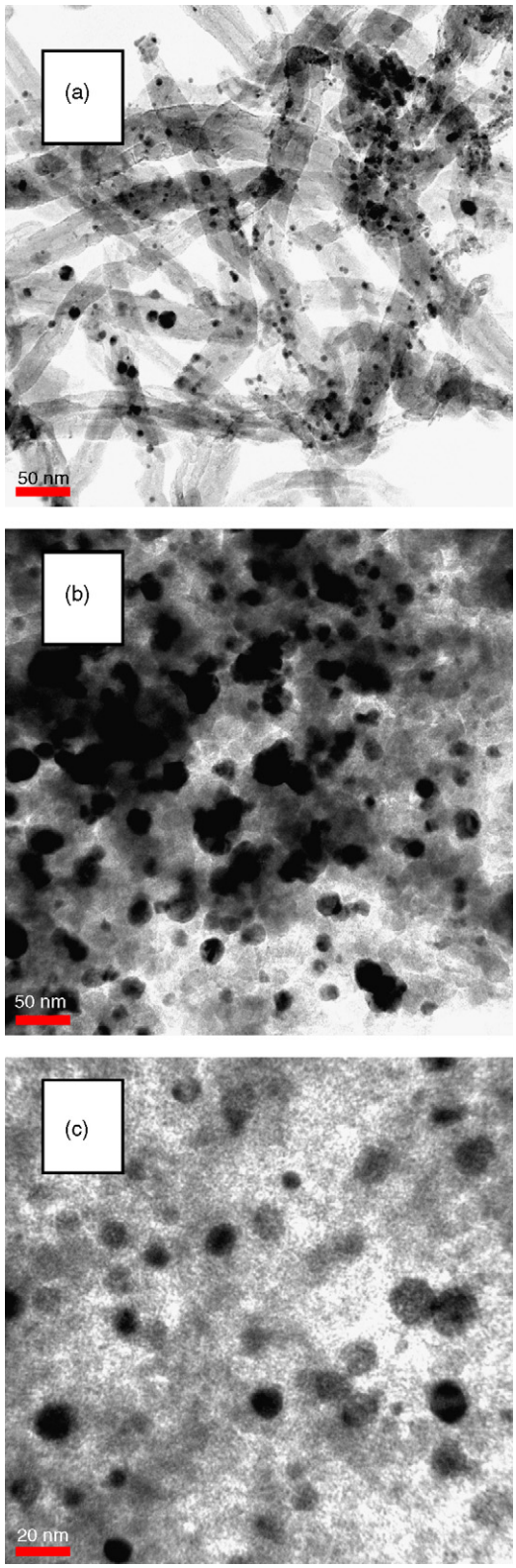

Fig. 2. TEM images of (a) Pd/MWCNT, (b) Pd/C and (c) Pd/ACF. Bars are 50 nm for images (a and b) and 20 nm for image (c).

100 mV more negative than that on Pt/C. This is the evidence that the kinetics of the ethanol oxidation on Pd/MWCNT is tremendously improved. It is an exception that Pd/ACF showed a poor performance for ethanol oxidation. We found that the adhesion of Pd on AFC is relatively poor. As shown in Fig. 1c that the coverage of Pd on AFC is very small which results in a lower active surface area for ethanol oxidation (see the CV in the inset of Fig. 4). These results demonstrated that the support plays an important role in the activity of Pd-based electrocatalyst for the oxidation of ethanol. The MWCNT as a support of

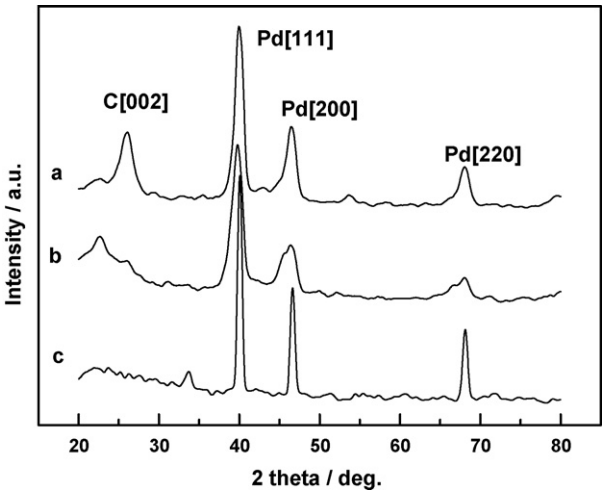

Fig. 3. XRD patterns of (a) Pd/MWCNT, (b) Pd/C and (c) Pd/ACF.

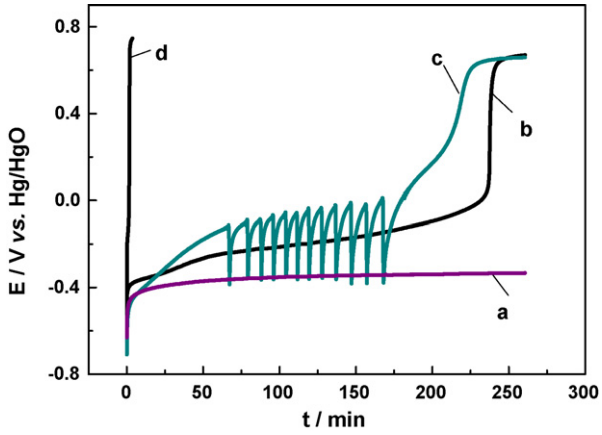

Fig. 5. Chronopotentiometric curves of ethanol oxidation on (a) Pd/MWCNT, (b) Pd/C, (c) Pt/C and (d) Pd/ACF at 1.0 mA cm^{-2} in 1 mol l^{-1} C_2H_5OH + 1 mol l^{-1} KOH solution.

Pd-based electrocatalyst for ethanol oxidation showed a better performance than that of carbon black support and ACFsupport.

Fig. 5 presents the chronopotentiometric curves of the ethanol oxidation on Pd/MWCNT, Pd/C, Pd/ACF and Pt/C electrocatalysts in 1 mol l^{-1} C_2H_5OH/1 mol l^{-1} KOH solution. The steady-state oxidation of ethanol on Pd/MWCNT electrode was performed at low potential and was very stable (Fig. 5a). The potential for ethanol oxidation on Pd/C electrode was also low, however, the potential increases with the time and final shifts to a higher potential for the oxygen evolution. In the case of Pt/C, the potential increases faster with the time. Potential oscillation appears during the polarization process and finally the potential shifts to a higher potential for oxygen evolution as well. This is a typical phenomenon of a poisoned electrocatalyst [21]. The poisoning of the electrocatalyst results in a larger potential polarization and then the poisoning species are oxidized at higher potentials to release the active sites for ethanol oxidation at lower potentials. The potential finally shifts to a higher value for oxygen evolution instead of ethanol oxidation, indicating the loss of activity for ethanol oxidation. The fact that no potential oscillation during the polarization process indicates that there was no strongly adsorbed species formed on the surface of Pd-based electrocatalysts to block the active sites for

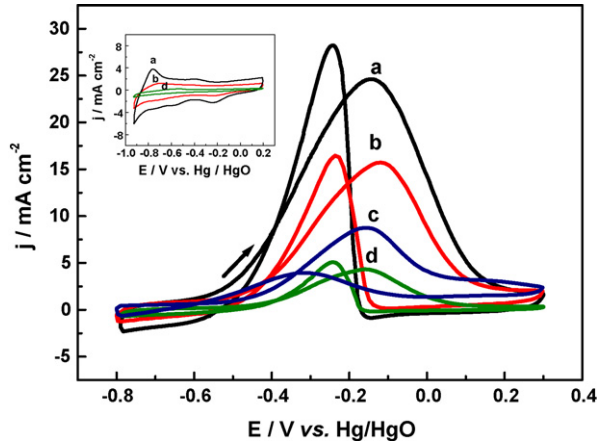

Fig. 4. Cyclic voltammograms of the Pd-based electrodes and Pt/C in 1 mol l^{-1} KOH solution containing 1 mol l^{-1} C_2H_5OH with sweep rate of 50 mV s^{-1} at room temperature, Pd loading: 0.2 mg cm^{-2}. (a) Pd/MWCNT, (b) Pd/C, (c) Pt/C and (d) Pd/ACF. Inset is the CVs of (a) Pd/MWCNT, (b) Pd/C and (d) Pd/ACF in 1 mol l^{-1} KOH solution without added ethanol.

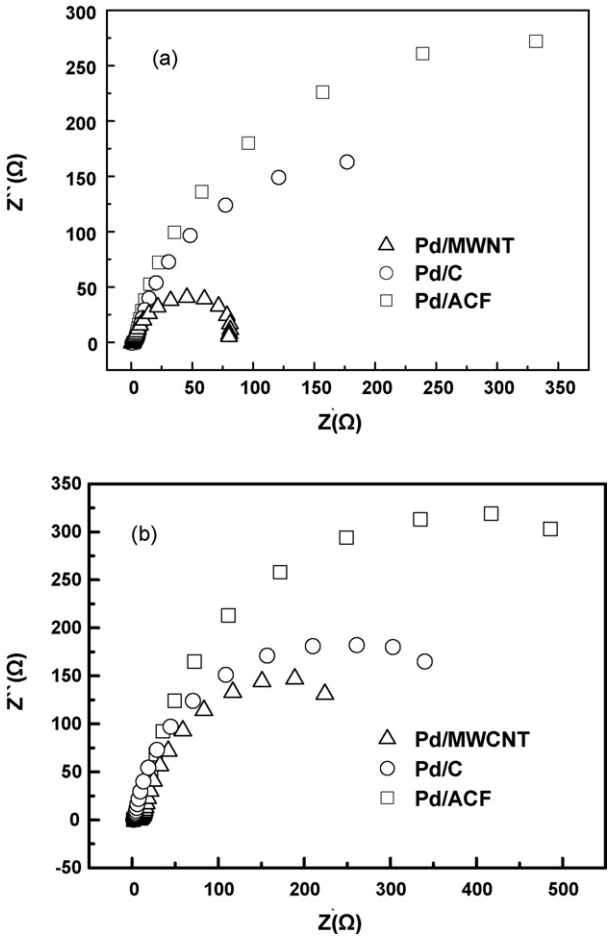

Fig. 6. Nyquist plots of EIS for ethanol oxidation on Pd/MWCNT, Pd/C and Pd/ACF electrodes in 1 mol l^{-1} KOH solution containing 1 mol l^{-1} C_2H_5OH at (a) −0.1 V and (b) −0.5 V vs. Hg/HgO. The frequencies are ranging from 10 K Hz to 0.1 Hz.

ethanol oxidation. As mentioned above, Pd/AFC is an exception that its performance is poor due to the very low electrocatalyst coverage (see Fig. 5d).

Electrochemical impedance spectroscopy (EIS) was used to compare the impedance characteristics of the different electrocatalysts. EIS measurements were carried out on Pd-based electrocatalysts at potentials of −0.5 and −0.1 V versus Hg/HgO. The corresponding Nyquist plots are shown in Fig. 6. The semicircle at high frequencies represents a charge transfer resistance (R) of main oxidation reaction. The reaction resistance decreases with the increase in the electrode polarization (from −0.5 to −0.1 V versus Hg/HgO). Fig. 6 shows a significant decrease of R for Pd/MWCNT at potentials of −0.5 and −0.1 V, indicating a smaller reaction resistance other than electrocatalysts. The smaller charge transfer resistance for Pd/MWCNT electrode has good correlation with the higher catalytic activity for ethanol oxidation in alkaline solution.

4. Conclusion

Pd-based electrocatalysts were prepared by an intermittent microwave heating technique. The properties of Pd electrocatalysts supported on different carbon materials including MWCNT, carbon black and AFC for ethanol oxidation were investigated by different electrochemical techniques along with the comparison to Pt/C electrocatalyst. Pd/MWCNT electrocatalyst showed the highest activity for ethanol oxidation in alkaline media. The results indicated that the support would significantly influence the catalytic activities of the Pd-based electrocatalysts for ethanol oxidation.

Acknowledgments

The authors gratefully acknowledge the support by the NNSFC (20476108, 50373053), the NSF of Guangdong Province (04105500), the Guangzhou Science and Technology Key Project (200523-D0251, 2005-ST-03) and the Guangdong Science and Technology Key Projects (2005A11001002, 2005A11004001).

References

[1] C. Lamy, A. Lima, V. LeRhun, F. Delime, C. Coutanceau, J.M. Léger, J. Power Sources 105 (2002) 283.
[2] S.Q. Song, P. Tsiakaras, Appl. Catal., B 63 (2006) 187.
[3] G. Tremiliosi-Filho, E.R. Gonzalez, A.J. Motheo, E.M. Belgsir, J.M. Léger, C. Lamy, J. Electroanal. Chem. 444 (1998) 31.
[4] S.L. Chen, M. Schell, J. Electroanal. Chem. 478 (1999) 108.
[5] E.V. Spinacé, A.O. Neto, M. Linardi, J. Power Sources 129 (2004) 121.
[6] G.A. Camara, R.B. de Lima, T. Iwasita, Electrochem. Commun. 6 (2004) 812.
[7] F. Vigier, C. Coutanceau, A. Perrard, E.M. Belgsir, C. Lamy, J. Appl. Electrochem. 34 (2004) 439.
[8] P.K. Shen, C.W. Xu, Electrochem. Commun. 8 (2006) 190.
[9] P.K. Shen, C.W. Xu, R. Zeng, Y.L. Liu, Electrochem. Solid-State Lett. 9 (2006) 39.
[10] W.Z. Li, C.H. Liang, J.S. Qiu, W.J. Zhou, H.M. Han, Z.B. Wei, G.Q. Sun, Q. Xin, Carbon 40 (2002) 787.
[11] R.P. Raffaelle, B.J. Landi, J.D. Harris, S.G. Bailey, A.F. Hepp, Mater. Sci. Eng., B 116 (2005) 233.
[12] T. Matsumoto, T. Omatsu, H. Nakano, K. Arai, Y. Nagashima, E. Yoo, T. Yamazaki, M. Kijima, H. Shimizu, Y. Takasawa, J. Nakamura, Catal. Today 90 (2004).
[13] W.Z. Li, C.H. Liang, W.J. Zhou, J.S. Qiu, Z.H. Zhou, G.Q. Sun, Q. Xin, J. Phys. Chem. B 1076 (2003) 292.
[14] X.S. Zhao, W.Z. Li, L.H. Jiang, W.J. Zhou, Q. Xin, B.L. Yi, G.Q. Sun, Carbon 42 (2004) 3251.
[15] M.F.R. Pereira, J.J.M. Órfão, J.L. Figueiredo, Carbon 40 (2002) 2393.
[16] F. Stoeckli, T.A. Centeno, A.B. Fuertes, J. Muniz, Carbon 34 (1996) 1201.
[17] Z.Q. Tian, S.P. Jiang, Y.M. Liang, P.K. Shen, J. Phys. Chem. B 110 (2006) 5343.
[18] S.X. Chen, H.M. Zeng, Carbon 41 (2003) 1265.
[19] Z.Q. Tian, F.Y. Xie, P.K. Shen, J. Mater. Sci. 39 (2004) 1507.
[20] Z.F. Liu, Z.Y. Shen, T. Zhu, S.F. Hou, L.Z. Ying, Z.J. Shi, Z.N. Gu, Langmuir 16 (2000) 3569.
[21] J.L. Rodríguez, R.M. Souto, L. Fernández-Mérida, E. Pastor, Chem. Eur. J. 8 (2002) 2134.